Kovove Mater. 51 2013 165–172
DOI: 10.4149/km_2013_3_165

Formation of nano-sized grains in Ti-10Zr-5Nb-5Ta biomedical alloy processed by accumulative roll bonding (ARB)

I. Cinca[1], D. Raducanu[1], A. Nocivin[2]*, D. M. Gordin[3], V. D. Cojocaru[1]

[1] *Politechnica University of Bucharest, Faculty of Materials Science and Engineering, 060042 Bucharest, Romania*
[2] *Ovidius University of Constanta, Faculty of Mechanical, Industrial and Maritime Engineering, 900527 Constanta, Romania*
[3] *Institut National des Sciences Appliques de Rennes, Rennes 35043, France*

Received 3 April 2012, received in revised form 9 October 2012, accepted 10 June 2013

Abstract

Formation of nano-sized grains in a new Ti-10Zr-5Nb-5Ta (wt.%) alloy without cytotoxic elements, through innovative accumulative roll bonding (ARB) process was the subject of investigation. The investigations consisted of structural and mechanical characterization of the alloy, processed by 4 ARB cycles at ambient temperatures. The micro-structural investigations were performed before and after each ARB cycle, using a SEM analyzing system, an X-ray diffractometer and a HRTEM analyzing system. The investigations of mechanical properties were based on tensile strength, Young's modulus, tensile elongation and micro-hardness measurements. Nano-sized grains were successfully obtained after 4 ARB cycles. The analyzed samples initially showed an ultra fine grain (UFG) structure, transformed during ARB cycles to a nano-sized grain (NG) structure, suitable for improving the alloy's bioactivity. Consequently, the ARB process increases the strength of the samples: the values of tensile strength drastically increase in the initial stage of the ARB process, after which they tend to become saturated; the Young's modulus constantly increases; the tensile elongation greatly decreases after 2 ARB cycles; the micro-Vickers hardness values are constantly high during ARB process.

K e y w o r d s: Ti-Zr-Nb-Ta alloy, grain refining, accumulative roll bonding, structure characterization, mechanical properties testing, nano-crystalline structure

1. Introduction

Actual tendencies in biomaterials and biomedical research areas are focused on new chemical compositions with advanced structures of Ti based alloys [1], other than commercial pure Ti (cp-Ti) and Ti-6Al-4V alloy. Unfortunately, the Ti-6Al-4V biomaterial, famous for its corrosion resistance and biocompatibility properties, has a negative long term performance, affected by Al and V liberation associated with the occurrence of serious health problems [2, 3], such as harming the haematopoietic system, developing Parkinson or Alzheimer disease and onset of neuropathy. This is the reason why the research concerning biometallic alloys is developing new chemical compositions of Ti based alloys, by including only non-toxic, biocompatible elements, such as Ta, Nb, Mo, Zr, in order to find new structures with advanced properties for biomedical applications [4, 5].

The present article proposes a promising biomedical alloy – Ti-10Zr-5Nb-5Ta (wt.%) – with a complex, multi-component chemical composition and without potentially cytotoxic elements, processed through an innovative ARB processing route. The ARB technology can assure a great grain refinement until nano-size crystalline structures are capable of increased bioactivity, which is essential for an implant biomaterial.

The ARB process developed by Saito et al. [6] represents one of several versions of severe plastic deformation (SPD) processing routes, by which ultra fine grains (UFG) and a nano-crystalline (NC) structure

*Corresponding author: tel./fax: +40241606431; e-mail address: anocivin@univ-ovidius.ro

Table 1. The rolling scheme of ARB procedure

No. of layers/ ARB cycle	Initial thickness of the sample package (mm)	Final thickness of the sample package (mm)	Final thickness of the obtained layers (mm)
2 – 1st cycle	0.20 (0.10 × 2)	0.15	approx. 0.075
4 – 2nd cycle	0.30 (0.15 × 2)	0.17	approx. 0.043
8 – 3rd cycle	0.34 (0.17 × 2)	0.18	approx. 0.023
16 – 4th cycle	0.36 (0.18 × 2)	0.19	approx. 0.012

can be obtained [7–11]. The ARB process involves the severe deformation of metallic sheets, without modification of overall material thickness. In real terms, this technique consists of plastic deformation by rolling two equally geometrical dimensioned stacked material sheets, with a deformation degree of 50 %. In these conditions, the final consolidated stacked sheet will have a final thickness equal to that of each original sheet before rolling. The ARB process can be applied on bulk materials and has a major advantage consisting in unlimited plastic deformations for an unlimited number of ARB cycles. Through this way, the grain dimensions decrease after each ARB cycle, until UFG or even NC dimensions are achieved.

Many research works [12, 13] state that the well known appealing qualities of the nano-scale material can improve properties such as bioactivity. Consequently, this present paper intends to associate a promising new bio-metallic alloy, obtained through ARB processing route, with NC structure capable of improved bioactivity.

2. Experimental procedure

2.1. ARB process

In order to obtain the Ti-10Zr-5Nb-5Ta (wt.%) alloy, a levitation melting technique with cold crucible, in a FIVES CELES MP 25 type furnace (215 kHz magnetic field frequency) was used. This technique is efficient in melting metals with very different melting points, without the risk of contamination, and also for obtaining ingots with high chemical homogeneity. In order to achieve a higher homogeneous microstructure, the samples used for ARB process were obtained through thermo-mechanical processing of the as-cast alloy. The thermo-mechanical process consisted of an initial cold-rolling deformation, followed by an annealing treatment. The cold-rolling deformation, accomplished with a total deformation degree of 85 % (thickness reduction), was performed on a MARIO DI MAIO LQR120AS laboratory mill. The annealing treatment, realized at 850 ℃, in argon atmosphere, with a maintaining time of 30 min and subsequent air cooling, was performed using a GERO SR 100 × 500 heat treatment laboratory oven.

The resulted sheet constitutes the precursor sample for ARB process. The precursor sample, used to initiate the ARB cycles, has been mechanically machined to $0.1 \times 8 \times 70\,\mathrm{mm}^3$ dimensions. Before each ARB cycle, the sample surfaces were degreased using an ultrasonic bath, for 5 min (ethylic alcohol at temperature of 60 ℃), in order to remove surface contamination and oxide scale. The ARB cycles were performed using the same aforementioned MARIO DI MAIO LQR120AS laboratory mill. Roll bonding was conducted with a rolling ratio of 50 %, so that the total thickness of the bonded sheet remained constant. In real terms, this technique consists of rolling two stacked metal sheets, with equal dimensions, using a deformation degree of 50 %, in order to obtain one final sheet with the same thickness like the original two ones. The ARB process was conducted up to 4 cycles at a rolling rate of 1.2 $\mathrm{m\,min}^{-1}$. The billet roll stand has been pre-tensioned for a negative skip (–0.2 mm). Table 1 presents the ARB rolling scheme. In the end of the ARB process, samples consisting in stacks of 4, 8 and 16 layers were selected for structural and mechanical investigations.

2.2. Micro-structural and mechanical characterization

The microstructures of the precursor sample and of the ARB processed samples were examined with: a QUANTA INSPECT F scanning electron microscope (SEM), with energy dispersive spectroscopy (EDS) analyzing system; a TECNAI F30 G^2 high resolution transmission electron microscope (HRTEM), with linear resolution of 0.1 nm and with point-resolution of 0.14 nm, using specimens prepared through ionic impact thinning; a PANalytical diffractometer with Bragg-Brentano geometry in 2θ, using a Cu K_α X-ray characteristic fascicle, with wavelength of 0.154065 nm.

The mechanical tests were realized as static tensile tests at ambient temperature, using the GATAN MICROTEST-2000 tensile module, and also the micro-hardness tester WILSON-WOLPERT 401MVA, located inside of the SEM-TESCAN VEGA II-XMU microscope.

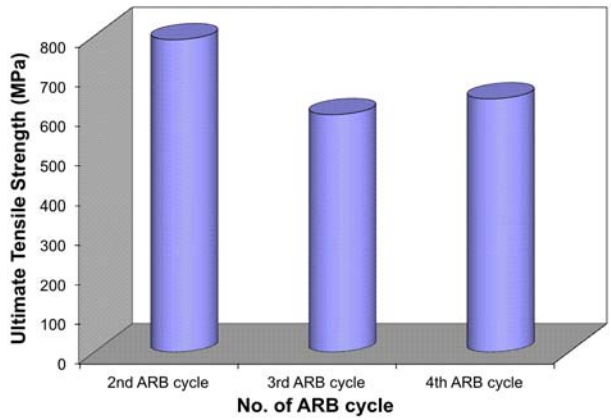

Fig. 1. Ultimate tensile strength of the Ti-10Zr-5Nb-5Ta alloy with ARB cycles.

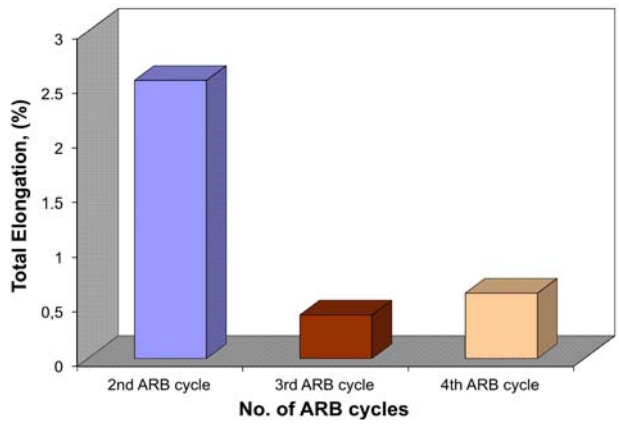

Fig. 3. Total elongation of the Ti-10Zr-5Nb-5Ta alloy with ARB cycles.

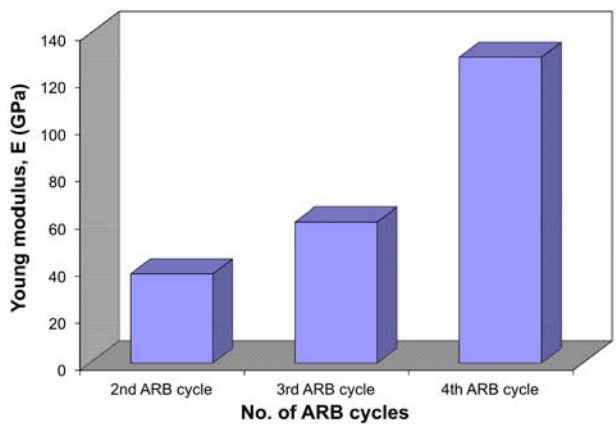

Fig. 2. Young's modulus of the Ti-10Zr-5Nb-5Ta alloy with ARB cycles.

3. Results and discussion

3.1. Mechanical properties of the ARB processed Ti-10Zr-5Nb-5Ta alloy

By processing the data from stress-strain diagrams resulted from tensile tests applied on samples with 4, 8 and 16 layers (2, 3 and 4 ARB cycles), the diagrams in Figs. 1, 2 and 3 have been obtained. These figures show the value variations of ultimate tensile strength (Fig. 1), Young's modulus (Fig. 2) and total elongation (Fig. 3) in accordance with the number of ARB cycle. In addition, Fig. 4 shows the values of the micro-hardness of the same samples. The results of the mechanically tested materials conduct to the following remarks and discussions:

Figure 1 shows the change in tensile strength values of the studied Ti alloy as a function of the number of ARB process cycles. The values corresponding to 2^{nd}, 3^{rd} and 4^{th} ARB cycles are indicated, which are most relevant to the evolution of mechanical properties. The tensile strength values increase in the initial stage (1 and 2 cycles) up to 790 MPa for the 2^{nd} ARB cycle, due to classical strain hardening mechanism of Hall-Petch method – smaller grain size will make the material harder. But after that, there is a slow decrease in the following two cycles (the 3^{rd} and 4^{th} ones) down to 600 MPa and 640 MPa, respectively, suggesting that in this stage of the ARB process, two possible phenomena can be taken into account, both discussed in specific literature and equally credible for the present case: The first one refers to an inverse Hall-Petch effect, observed for nano-crystalline materials and reported by a large number of papers. This effect refers to the fact that nano-crystalline materials get softer as grain size is reduced below a critical value, due to dislocations based models or grain-boundary-shearing models [14]. The second possible phenomenon refers to dynamic recovery of heavily deformed structure which may occur. During the ARB process, due to drastic plastic deformations, the temperature of the samples could forcefully rise, even if the process was conducted at room temperature [15, 16]. In these conditions, a partial dynamic recovery can develop during higher ARB cycles, which can lead to a diminution of the strain hardening. This behavior has also been reported in some Al and other Ti based alloys [17, 18].

Figure 2 shows the variations of the Young's modulus values for the studied alloy samples in accordance with ARB cycles. In this case, there is a constant increase of these values during ARB process, due to the strain hardening of the alloy. The dynamic recovery phenomenon, suggested above, apparently does not affect the modulus in this stage of the ARB process. Clearly, it must be inferred that the two discussed phenomena – strain hardening and possible dynamic recovery – have a competition influence on the alloy structure, even in these early stages of ARB process.

Figure 3 shows the variations of the total elongation values for the studied samples of the alloy in

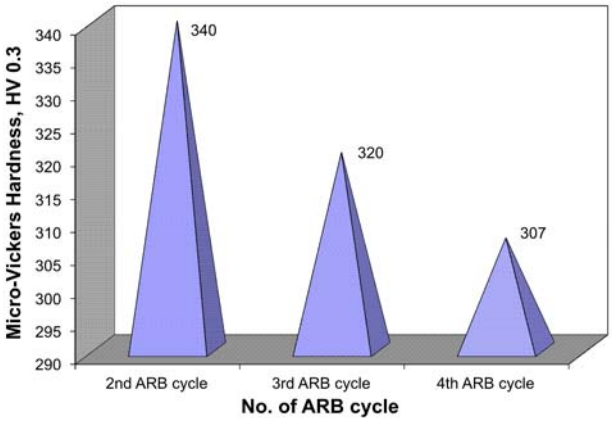

Fig. 4. Micro-Vickers hardness of the Ti-10Zr-5Nb-5Ta alloy with ARB cycles.

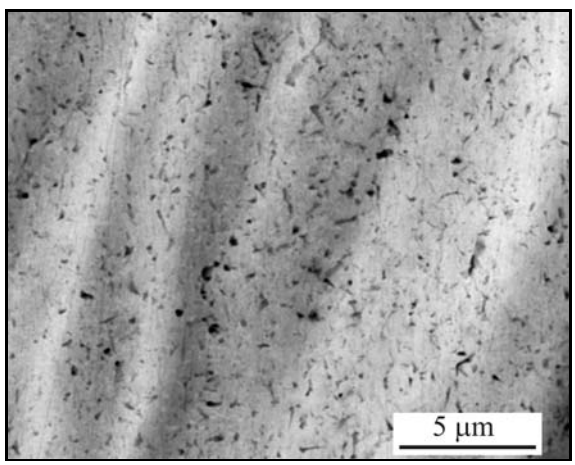

Fig. 5. SEM image of the precursor sample, before ARB process, thermo-mechanically treated: fine equiaxed grains of β phase, with inter-granular fine micro-zones of α phase.

accordance with the ARB cycles (the measurement length on sample (L_o) for calculation of elongation was $L_o = 70$ mm). Here, the value from the 2nd ARB cycle (2.55 %) suddenly decreases in the 3rd cycle to 0.4 %, suggesting the strain hardening phenomena, after which it slowly increases to 0.6 % in the 4th cycle. The same analysis is valid for Fig. 4, which shows the variations of the micro-Vickers hardness values for the studied samples of the alloy in function of ARB cycles. The micro-hardness values are slowly decreasing with ARB cycles, from 340 $HV_{0.3}$ to 320 $HV_{0.3}$, and finally to 307 $HV_{0.3}$, suggesting the inverse Hall-Petch effect or the partial dynamic recovery phenomena.

However, beside mechanical properties evolution in the alloy structure, the main and most desired phenomenon of the ARB process is the grain size diminution that can be highlighted and analyzed by structural characterization of the newly studied alloy.

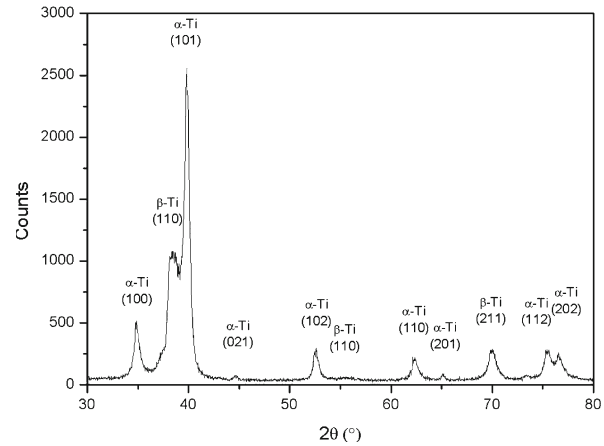

Fig. 6. XRD spectra of the precursor sample before ARB process.

3.2. Structural analysis of the ARB processed Ti-10Zr-5Nb-5Ta alloy – Formation of the nano-sized grains

In order to highlight the diminution of the grain size during ARB process, the structural analysis of the studied Ti alloy began with the analysis of the precursor sample for establishing the initial structural characteristics before the ARB process. The microstructural features of the precursor sample, after a cold rolling deformation and an annealing treatment, are visible in Fig. 5. Figure 5 shows beside traces of material deformation lines, a micro-structure formed by equiaxed grains of β cubic phase, separated by inter-granular α hexagonal phase (dark zones). The presence of these two phases is confirmed by XRD patterns from Fig. 6. In addition, XRD spectra also indicate traces of TiO_2, existent on the sample surface, which have been brushed aside before the start of the ARB process, through a degreasing procedure described above in the experimental procedure. The average dimension of the equiaxed grains of the precursor sample is about 350–400 nm.

Figures 7, 8, 9 correspond to Ti-10Zr-5Nb-5Ta alloy after ARB cycles 2, 3 and 4, representing the most delineative SEM images of the samples with 4, 8 and 16 layers, respectively. All SEM images indicate a general micro-structural aspect referring to the bi-phase structure ($\alpha + \beta$), presented and detected in all samples of investigated Ti-10Zr-5Nb-5Ta (wt.%) alloy: fine β grains with small quantities of inter-granular α phase at grain boundaries (dark zones). The X-ray diffraction analysis confirms the presence of two phases (α and β) in all 3 stages of ARB process studied (2nd, 3rd and 4th ARB cycles). Only the XRD spectra for the 16 layer sample (4 ARB cycles) indicated in Fig. 10 were selected as presentation, which is the most representative for the purpose of this present

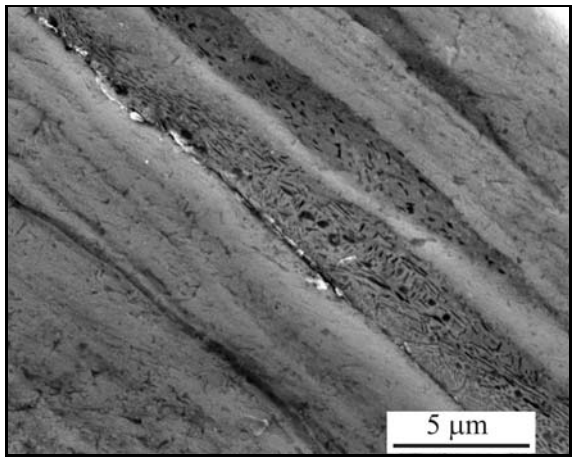

Fig. 7. SEM image for the sample after 2 ARB cycles (4 layers); the material orientation on deformation direction, and the non-uniformity of the adhesion zones between layers are visible.

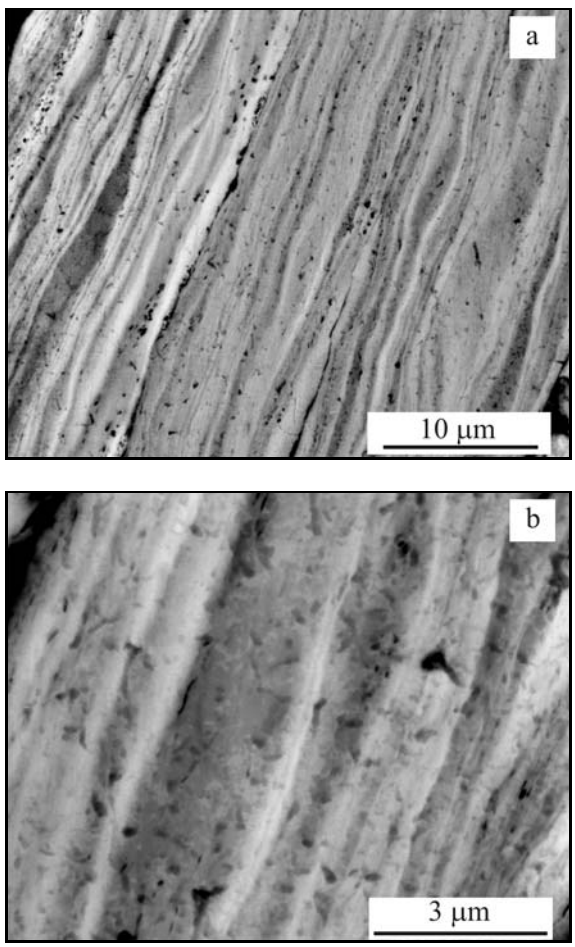

Fig. 8. SEM images at different magnifications for the sample with 8 layers (after 3 ARB cycles): (a) good adhesion between layers is visible; (b) fine equiaxed crystallites of β phase and inter-granular α phase.

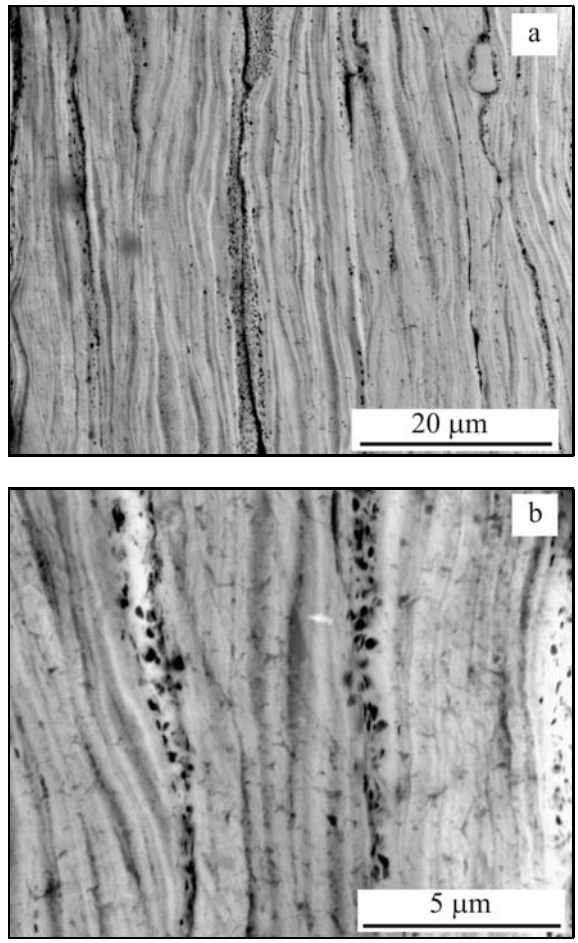

Fig. 9. SEM images at different magnifications for the sample with 16 layers (after 4 ARB cycles): (a) good adherence between layers; drastic material deformation; (b) equiaxed nano-scale grains of β phase and inter-granular α phase.

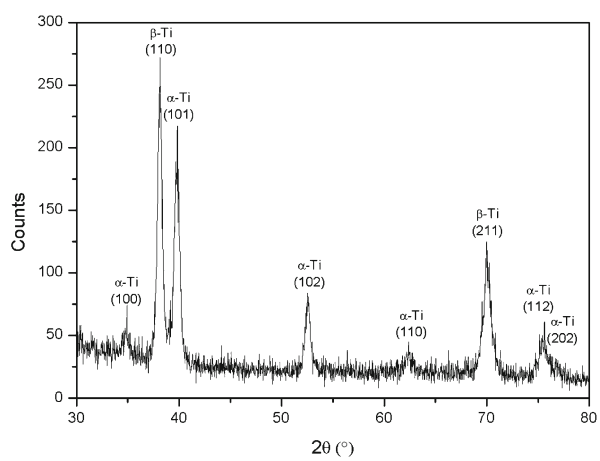

Fig. 10. XRD spectra of the 16 layers – ARB processed sample; the presence of α and β phases.

paper because of finer grain dimensions obtained during ARB process, attested by the most flattened patterns. There are some important micro-structural particularities of each ARB processed sample. Figure 7, corresponding to SEM image of the sample after 2 ARB cycles (4 layers), shows hard material deformation along rolling direction and a non-uniformity of the adhesion zones between layers. The micro-structure is characterized by coarse grains of the separation zones between layers, finer crystallites of β phase and the inter-granular network of α phase in the middle layers. Average dimension of the fine crystallites is about 250–300 nm, thinner than that of the precursor sample. The equiaxed grain shape argues the beginning of the dynamic recovery, suggested in the analysis part of the mechanical properties, but, correlated with the high tensile strength from this stage, it is evident that the strain hardening phenomena is more powerful in this stage of the ARB process than the dynamic recovery. Figure 8 represents two SEM images at different magnifications of the sample with 8 layers (after 3 ARB cycles). Figure 8a shows a good adhesion between layers, comparative to earlier stage, and Fig. 8b, realized at a higher magnification, a thinner grain size, of about 200 nm. Figure 9 also represents two SEM images at different magnifications, but pertaining to the sample with 16 layers (after 4 ARB cycles). Also, a good adherence is visible between layers and as well as a drastic material deformation (Fig. 9a). Figure 9b shows fine equiaxed crystallites of about 10 nm.

For the sample with 8 layers (third ARB stage), the elongation decrease with the tensile strength is comparable to corresponding values of earlier stages. This suggests that at higher strains (beginning with third cycle) the strain hardening mechanism, specific for hard deformation processes, is possibly gradually attenuated by dynamic recovery, attested by the equiaxed shape of the grains. However, future researcher works must focus on this fact. The most important fact is that the grain sizes decrease continuously, even if the Young's modulus continues to increase and total elongation decreases. Once achieving the nano-metric size of the grains, mechanical properties can be improved by subsequent annealing treatments.

Figure 11 shows the grain size refinement during ARB process, applied on the Ti-10Zr-5Nb-5Ta studied alloy, compared with precursor sample. The drastic diminution of the grain size after 4 ARB cycles is visible. The size of approximately 10 nm represents a promising value for future investigations of the bioactivity of the newly studied Ti-10Zr-5Nb-5Ta alloy.

For this most important sample, corresponding to 4 ARB cycles, with a grains size of about 10 nm, the micro-structural analysis has been detailed by performing HRTEM microscopy. Observed structural aspects revealed a highly tensioned structure, a fact

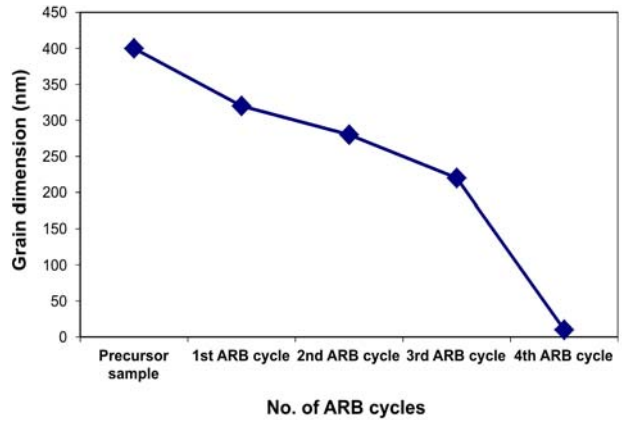

Fig. 11. The decrease of the grain dimension of the Ti-10Zr-5Nb-5Ta alloy as a function of ARB cycles.

which is highlighted by the presence of the characteristic contrast lines, visible in Fig. 12a. Figure 12b reveals the obtained nano-metric crystalline structure, with crystallites measuring around 7–12 nm (7.8 nm, 11.4 nm and 11.6 nm). At such a small grain size it is suggested that the microstructure presents a timid beginning of an amorphization process. Miller indices for some families of lattice planes and the corresponding inter-planar distance were also detected and measured: (110) Miller indices for β-Ti phase, with inter-planar distance of 2.32 Å and (101) Miller indices for α-Ti phase with inter-planar distance of 2.24 Å (Fig. 12c). Figure 12 confirms the advantage of ARB procedure in decreasing the grain dimension, which also represents a promising result as the way of obtaining structures at a nano-scale for new proposed multi-component Ti alloy.

4. Conclusions

The aim of the present work was to obtain nano-size grains for a newly proposed Ti-10Zr-5Nb-5Ta alloy, by applying the ARB process, without the presence of potentially cytotoxic elements, in order to improve the alloy's bioactivity. 4 ARB cycles were applied. The obtained samples were mechanically tested and also structurally characterized using SEM, XRD and HRTEM techniques.

The main objective of the research work was achieved by obtaining a diminution of the grain size between 350–400 nm, before ARB process, for the precursor sample, to 10 nm, after applying 4 ARB cycles.

The investigation of mechanical properties indicates an increase of tensile strength values in the 1st and 2nd ARB cycle, followed by a slow decrease beginning with 3rd ARB cycle, due to strain hardening phenomena in the beginning, followed by possible inverse Hall-Petch effect or possible dynamic recov-

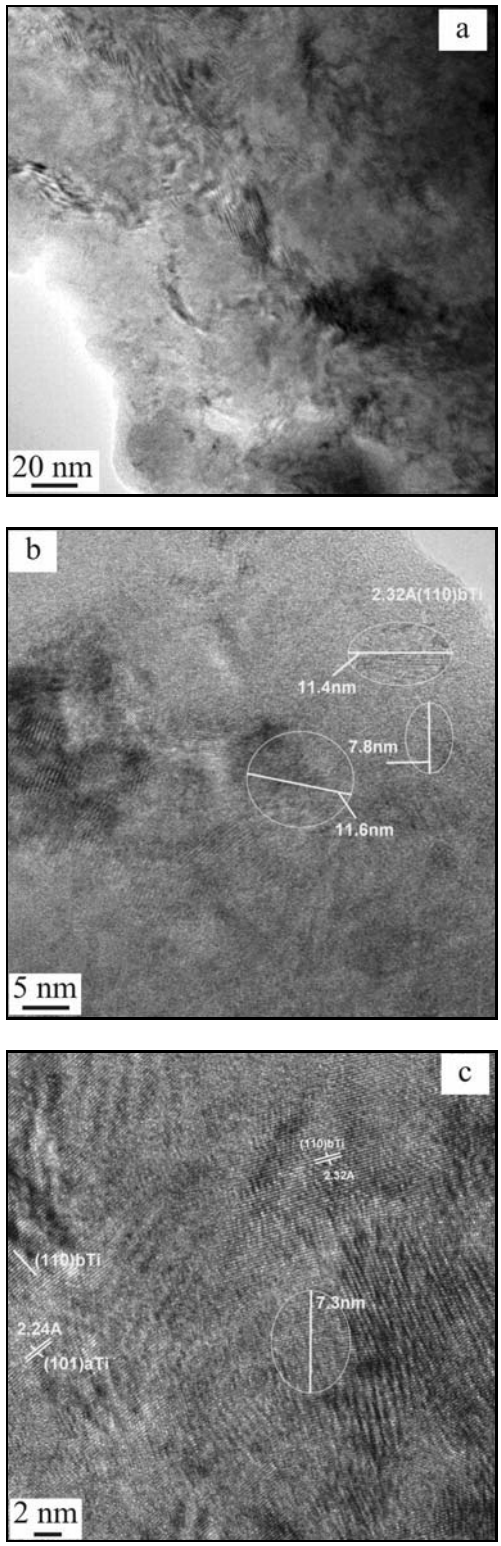

Fig. 12. HRTEM images of 16 layers – ARB processed sample: (a) high tensioned nano-sized structure, spotlighted by the presence of characteristic contrast lines; (b) high tensioned nano-crystalline structure, with contrast lines and measured grain dimension; (c) the Miller indices for β-Ti and α-Ti phases, with measured inter plane distance.

ery phenomenon, a fact which must be focused and developed by future researchers. The Young's modulus increases and the total elongation decreases during all ARB process, suggesting that the strain hardening phenomenon is more prominent than the dynamic recovery, which visibly affects only the grain shape being equiaxed.

The micro-structural investigations reveal the presence of two phases, β cubic phase (in majority) and α hexagonal phase, a good adherence between layers for the 3rd and 4th ARB cycles, and a constant decrease of the grain size of the present crystallites, with timid beginning of an amorphization process in the 4th ARB stage.

The advantage of the ARB procedure in decreasing the grain dimension was confirmed: crystallite dimensions for ARB processed sample with 16 layers are around 7–11 nm, which values represent a promising result as a way of obtaining structures at a nano-scale for a multi-component Ti alloy, suitable for improving the alloy's bioactivity.

Acknowledgements

This work has been funded by the Operational Program of Human Resources Development 2007–2013 of the Romanian Ministry of Labor, Family and Social Protection through the Financial Agreement POSDRU/6/1.5/S/16.

References

[1] Geetha, M., Singh, A. K., Asokamani, R., Gogia, A. K.: Prog Mater Sci, *54*, 2009, p. 397. doi:10.1016/j.pmatsci.2008.06.004

[2] Ngwa, H. A., Kanthasamy, A., Anantharam, V., Song, C., Witte, T., Houk, R. S., Kanthasamy, A. G.: Toxicol Appl Pharmacol, *240*, 2009, p. 273.

[3] Donato, T. A. G., de Almeida, L. H., Nogueira, R. A., Niemeyer, T. C., Grandini, C. R., Caram, R., Schneider, S. G., Santos, Jr., A. R.: Mater Sci Eng C, *29*, 2009, p. 1365. doi:10.1016/j.msec.2008.10.021

[4] Bertrand, E., Gloriant, T., Gordin, D. M., Vasilescu, E., Drob, P., Vasilescu, C., Drob, S. I.: J Mech Behav Biomed Mater, *3*, 2010, p. 559. PMid:20826361. doi:10.1016/j.jmbbm.2010.06.007

[5] Bhola, S. M., Bhola, R., Mishra, B., Olson, D. L.: J Mater Sci, *45*, 2010, p. 6179. doi:10.1007/s10853-010-4711-1

[6] Saito, Y., Tsuji, N., Utsunomiya, H., Hong, R. G.: Scripta Mater, *39*, 1998, p. 1221. doi:10.1016/S1359-6462(98)00302-9

[7] Raducanu, D., Vasilescu, E., Cojocaru, V. D., Cinca, I., Drob, P., Vasilescu, C., Drob, S. I.: J Mech Behav Biomed Mater, *4*, 2011, p. 1421. PMid:21783152. doi:10.1016/j.jmbbm.2011.05.012

[8] Hausöl, T., Maier, V., Schmidt, C. W., Winkler, M., Höppel, H. W., Göken, M.: Adv Eng Mater, *12*, 2010, p. 740. doi:10.1002/adem.201000044

[9] Terada, D., Inoue, S., Tsuji, N.: J Mater Sci, *42*, 2007, *42*, p. 1673. doi:10.1007/s10853-006-0909-7
[10] Shaarbaf, M., Totoghinejad, M. R.: Metal Mater Trans A, *40A*, 2009, p. 1693. doi:10.1007/s11661-009-9851-z
[11] Semenova, I. P., Valiev, R. Z., Yakushina, E. B., Salimgareeva, G. H., Lowe, T. C.: J Mater Sci, *43*, 2008, p. 7354. doi:10.1007/s10853-008-2984-4
[12] Gordin, D. M., Gloriant, T., Texier, G., Thibon, I., Ansel, D., Duval, J. L., Nagel, M. D.: J Mater Sci: Mater Med, *15*, 2004, p. 885. PMid:15477740. doi:10.1023/B:JMSM.0000036276.32211.31
[13] Yamaguchi, S., Takadama, H., Matsushita, T., Nakamura, T., Kokubo, T.: J Mater Sci: Mater Med, *21*, 2010, p. 439. PMid:15477740. doi:10.1007/s10856-009-3904-0
[14] Carlton, C. E., Ferreira, P. J.: Acta Mater, *55*, 2007, p. 3749. doi:10.1016/j.actamat.2007.02.021
[15] Tsuji, N., Toyoda, T., Minamino, Y., Koizumi, Y., Kiritani, M., Komatsu, M.: Mater Sci Eng A, *350/1–2*, 2003, p. 108. doi:10.1016/S0921-5093(02)00709-8
[16] Lim, C. Y., Han, S. Z., Lee, S. H.: Metal Mater Inter, *12*, 2006, p. 225. doi:10.1007/BF03027535
[17] Horita, Z., Smith, D. J., Furukawa, M., Nemoto, M., Valiev, R. Z., Langdon, T. G.: J Mater Res, *11*, 1996, p. 1880. doi:10.1557/JMR.1996.0239
[18] Oh-ishi, K., Horita, Z., Smith, D. J., Furukawa, M., Valiev, R. Z., Nemoto, M., Langdon, T. G.: J Mater Res, *14*, 1999, p. 4200. doi:10.1557/JMR.1999.0569